ANNALS of Clinical and Translational Neurology
Open Access
ANA American Neurological Association since 1875

RESEARCH ARTICLE

Dysregulation of 14-3-3 proteins in neurodegenerative diseases with Lewy body or Alzheimer pathology

Michael B. McFerrin[1], Xiaofei Chi[2,*], Gary Cutter[2] & Talene A. Yacoubian[1]

[1]Department of Neurology, Center for Neurodegeneration and Experimental Therapeutics, University of Alabama at Birmingham, Birmingham, Alabama
[2]Department of Biostatics, University of Alabama at Birmingham, Birmingham, Alabama

Correspondence
Talene A. Yacoubian, Civitan International Research Center 560D, 1719 6th Avenue South, Birmingham, AL 35294.
Tel: 1 205 996 7543; Fax: 1 205 996 6580;
E-mail: tyacoub@uabmc.edu

Present address
*Department of Biostatistics, University of Arkansas for Medical Sciences, Little Rock, Arkansas

Funding Information
This work was supported by the Michael J. Fox Foundation for Parkinson's Research, the National Institute of Neurological Disorders and Stroke (R01 NS088533), and the Parkinson's Association of Alabama.

Received: 20 December 2016; Revised: 13 April 2017; Accepted: 17 April 2017

Annals of Clinical and Translational Neurology **2017; 4(7): 466–477**

doi: 10.1002/acn3.421

Abstract

Objective: The highly conserved 14-3-3 proteins interact with key players involved in Parkinson's disease (PD) and other neurodegenerative disorders. We recently demonstrated that 14-3-3 phosphorylation is increased in PD models and that increased 14-3-3 phosphorylation reduces the neuroprotective effects of 14-3-3 proteins. Here, we investigated whether 14-3-3 phosphorylation is altered in postmortem brains from control, PD, Alzheimer's Disease (AD), Alzheimer's with Lewy Bodies (ADLB), Dementia with Lewy Bodies (DLB), and Progressive Supranuclear Palsy (PSP) subjects at three conserved sites: serine 58 (S58), serine 185 (S185), and serine 232 (S232). **Methods**: S58, S185, and S232 phosphorylation was measured by western blot analysis of Triton X-100 soluble and insoluble fractions from postmortem temporal cortex. **Results**: The ratio of soluble phospho-S232 to insoluble phospho-S232 was reduced by 32%, 60%, 37%, and 52% in PD, AD, ADLB, and DLB, respectively. S185 and S58 phosphorylation were mildly elevated in the soluble fraction in DLB. We also noted a dramatic reduction in soluble pan 14-3-3 levels by ~35% in AD, ADLB, and DLB. Lower ratios of soluble to insoluble S232 phosphorylation (pointing to higher insoluble pS232) correlated with lower soluble pan 14-3-3 levels, suggesting that S232 phosphorylation may promote insolubilization of 14-3-3s. The phospho-S232 ratio and soluble pan 14-3-3 levels correlated with clinical and pathological severity. **Interpretation**: These data reveal dysregulation of 14-3-3 proteins in neurodegeneration associated with Lewy body or Alzheimer pathology. S232 phosphorylation may drive insolubilization of 14-3-3s and thus contribute to the pathophysiology in neurodegenerative disorders associated with Lewy body or Alzheimer pathology.

Introduction

14-3-3 proteins comprise a family of seven highly conserved proteins in mammals involved in cellular functions important to neuronal function, including protein folding, protein trafficking, neurite growth, and cell survival.[1–6] 14-3-3s have been linked to neurodegeneration. Several proteins implicated in Parkinson's disease (PD), including alpha-synuclein (αsyn), leucine-rich repeat kinase 2 (LRRK2), and parkin, interact with 14-3-3s[7–11], and 14-3-3s colocalizes with αsyn in Lewy bodies, the primary pathological hallmark of PD.[12,13] Expression of several 14-3-3 isoforms is reduced in αsyn models.[14,15] We have shown that 14-3-3 overexpression, particularly 14-3-3θ, is protective in neurotoxin, αsyn, and LRRK2 models of PD, while 14-3-3 inhibition promotes toxicity in these models.[5,15–17] 14-3-3s also interact with proteins implicated in other neurodegenerative disorders, including beta-amyloid (Aβ), tau, superoxide dismutase, and huntingtin.[18–22] 14-3-3s colocalize with these aggregation-prone proteins in neurofibrillary tangles and plaques of Alzheimer's disease (AD), Huntington's disease (HD) inclusion bodies, and inclusions observed in amyotrophic lateral sclerosis (ALS).[20,23–25]

Phosphorylation of 14-3-3s is a well-recognized mechanism for regulating 14-3-3 function. There are three

conserved phosphorylation sites on 14-3-3s: serine 58 (S58), serine 185 (S185), and serine/threonine 232 (S232). Not all isoforms have all three phosphorylation sites. S58 is present in all isoforms except 14-3-3σ and θ; S185 is present in 14-3-3β, ε, σ, and ζ; and S/T232 is limited to 14-3-3θ and ζ. Phosphorylation at S58 regulates 14-3-3 dimerization,[26] while phosphorylation at S185 regulates ligand binding.[27,28] Phosphorylation at either site causes release of proapoptotic factors and cell death.[27–29] Phosphorylation at S232 likely impacts ligand binding as the C-terminal tail can fold back to block the binding pocket.[30] We observed alterations in 14-3-3 phosphorylation in several PD models.[31] S232 phosphorylation of 14-3-3θ increased in rotenone-treated neuroblastoma cells and in cells overexpressing αsyn.[31] S58 phosphorylation was also increased in the rotenone model.[31] Mutation of S232 affected 14-3-3θ's neuroprotective effects against rotenone and 1-methyl-4-phenylpyridinium (MPP^+), with the phosphomimetic S232D mutant lacking any protective effect compared to wildtype or S232A 14-3-3θ.[31] The phosphomimetic S58D also reduced the protective effect of 14-3-3ζ against neurotoxins.[31] These mutational studies suggest that phosphorylation at S58 and S232 may promote neurodegeneration in PD.

In this study, we examined 14-3-3 phosphorylation in human PD and other neurodegenerative disorders. We surveyed Triton X-100 soluble and insoluble fractions of postmortem temporal cortices of control, PD, AD, Alzheimer's with Lewy Bodies (ADLB), Dementia with Lewy Bodies (DLB), and Progressive Supranuclear Palsy (PSP) subjects for 14-3-3 phosphorylation at all three sites. We also surveyed total 14-3-3 expression levels. We found evidence for enhanced phosphorylation and reduced solubility of 14-3-3 proteins in these disorders, and associations between these changes and clinical and pathological severity.

Experimental Procedures

Materials

Primary antibodies included rabbit polyclonal antibody against pan 14-3-3 isoforms (Abcam #ab6081, Cambridge, MA), mouse monoclonal antibody against pan 14-3-3 isoforms (Santa Cruz #sc-1657, Dallas, TX), mouse monoclonal antibody against 14-3-3θ (Abcam #ab10439), rabbit polyclonal antibody against phospho-S58 (pS58) 14-3-3 (Abcam #ab51109), rabbit polyclonal antibody against phospho-S232 (pS232) 14-3-3θ (Abcam #ab63369), sheep polyclonal antibody against phospho-S185 (pS185) 14-3-3 (ENZO Life Science #SA-479, Farmingdale, NY), and rabbit monoclonal antibody against phospho-S129 αsyn (Abcam #ab168381). Horseradish peroxidase-conjugated secondary antibodies were goat anti-rabbit and goat anti-sheep (Jackson Immunoresearch, West Grove, PA). Fluorescent-conjugated secondary antibodies used were IRDye 800CW donkey anti-rabbit and IRDye 680RD donkey anti-mouse (LI-COR Biotechnology, Lincoln, NE).

Human brain sample preparation

Fresh-frozen tissue from temporal cortices of age and gender-matched control, PD, AD, ADLB, DLB, and PSP brains were obtained from Banner Sun Health Research Institute Brain and Body Donation Program. Samples were homogenized in lysis buffer (50 mmol/L Tris-HCl pH 7.4, 175 mmol/L NaCl, 5 mmol/L EDTA) supplemented with protease and phosphatase inhibitors and sonicated for 10 sec on ice. After addition of Triton X-100 to a final concentration of 1% v/v, samples were incubated on ice for 30 min and centrifuged at 15,000xg for 60 min at 4°C. The supernatant was saved as the Triton X-100 soluble fraction. The pellet was resuspended in lysis buffer with 2% SDS, sonicated for 10 sec, and centrifuged for 5 min at 15,000*g*. The resulting supernatant was reserved as the Triton X-100 insoluble fraction.

Western blotting

Human brain lysates were separated on 26-well precast 12% SDS-PAGE gels with at least four samples from each disease group per gel. Several replicate gels were run simultaneously to assess the three phosphorylation sites and total 14-3-3 levels by western blot. Total protein loaded was visualized using EZBlue Protein Gel Stain (Sigma, St. Louis, MO). Proteins were transferred to PVDF membranes and blocked in a solution of 1:1 Odyssey blocking buffer in TBS-T (25 mmol/L Tris-HCl (pH 7.6), 137 mmol/L NaCl, 0.1% Tween 20) for 1 h. Membranes were incubated in primary antibodies in blocking buffer for a minimum of 4 h at 4°C followed by washes in TBS-T. Secondary antibodies were applied to the membranes in blocking buffer for one hour and washed 4 × 10 min in TBS-T. Pan 14-3-3, pS58, and pS185 were imaged using horseradish peroxidase-conjugated secondary antibodies and Pierce ECL Western blotting substrate (Thermo Fisher) and exposed to film. Total 14-3-3θ and pS232 were imaged using fluorescent secondary antibodies on a LICOR Odyssey Imaging system.

Immunohistochemistry

Forty micrometer free-floating sections from the temporal cortex of control brains and brains with pathological

diagnoses of PD and AD were obtained from Banner Sun Health Research Institute Brain and Body Donation Program. Sections were washed in PBS with Triton ×-100 (PBS-Tx 0.025%) and incubated with 1% H2O2 in PBS-Tx for 30 min to suppress endogenous peroxidase. After three washes in PBS-Tx, sections were blocked in 10% normal goat serum in PBS-Tx and incubated in primary antibody in PBS-Tx overnight. Sections were washed three times in PBS-Tx and incubated in horseradish peroxidase-conjugated secondary antibodies diluted in PBS-Tx. Sections were washed in PBS-Tx twice and then in Tris solution prior to reaction in DAB solution for about 45 sec. Sections were subsequently stained with 0.1% cresyl violet solution.

Aβ ELISA

Aβ levels in human brain lysates were measured using an ELISA for Aβ42 (EMD Millipore #EZBRAIN42, Billerica, MA), according to manufacturer's instructions.

Data analysis

Western blots exposed to film were scanned and analyzed using Un-Scan-It 6.1 gel analysis software, and images obtained from the LICOR imaging system were analyzed using Image Studio Lite 4.0. PS58 and pS185 were normalized to pan 14-3-3 levels, while pS232 was normalized to total 14-3-3θ. While 14-3-3ζ can be phosphorylated at the homologous T233, the pS232 antibody was specific to the 14-3-3θ isoform, as we previously demonstrated.[31] Total 14-3-3θ and pan 14-3-3 levels were normalized to total protein loading as determined by EZBlue Protein Gel staining. Values were normalized to the average of the control values for each blot.

Descriptive statistics were computed, and normality and outlier tests were performed for biochemical measures. Analysis of variance (ANOVA) was used to examine differences in 14-3-3 phosphorylation ratios across groups. Dunnett's multiple comparison test was used for post hoc analyses to identify which groups differed from control. Stepwise linear regression models were fitted for each 14-3-3 measure to assess differences among groups after adjusting for possible confounders, including gender, age, last Mini Mental Status Examination (MMSE) score, motor United Parkinson's Disease Rating Scale (UPDRS) score, and pathological measures (plaque density scores, tangle density scores, and Lewy-related histopathology scores). Nominal *P*-values of 0.05 were used in these confirmatory analyses with no multiple comparisons adjustments. All analyses were conducted using SAS software (Version 9.4, SAS Institute).

Results

14-3-3θ phosphorylation at serine 232 is altered in neurodegenerative disorders associated with Lewy body or Alzheimer pathology

Western blots were performed on Triton X-100 soluble and insoluble fractions of postmortem human temporal cortex samples from control, PD, AD, ADLB, DLB, and PSP subjects to test for changes in 14-3-3 phosphorylation at S58, S185, and S232 (Figs. 1, S1). Table 1 provides descriptive statistics of the sample populations. The most dramatic changes were observed in S232 phosphorylation of 14-3-3θ (Fig. 1A). S/T232 is present in 14-3-3θ and ζ, but the antibody used here is specific to S232 phosphorylation of 14-3-3θ, as we previously showed.[31] The Triton X-100 soluble fraction showed significant reduction in pS232 levels in AD (44%), ADLB (28%), and DLB (34%), with a nonsignificant decrease in pS232 phosphorylation in PD of 16% ($P = 0.099$) (Fig. 1A). Conversely, the Triton X-100 insoluble fraction showed a significant increase in S232 phosphorylation in PD (37%), AD (43%), and DLB (42%) (Fig. 1A).

At S58, which can be phosphorylated in most isoforms, there was increased phosphorylation in DLB (39%) in the soluble fraction (Fig. 1B). There were no significant changes at S58 in the insoluble fraction (Fig. 1B). S185 phosphorylation (found in 14-3-3β, ε, σ, and ζ) was significantly increased in DLB by 44% in the soluble fraction (Fig. 1C). S185 phosphorylation in the insoluble fraction was significantly increased in ADLB by 30% (Fig. 1C).

Total soluble 14-3-3 levels are reduced in several neurodegenerative diseases

We also evaluated total 14-3-3θ and pan 14-3-3 protein levels across all diseases in Triton X-100 soluble and insoluble fractions. The insoluble fraction showed significantly increased levels of 14-3-3θ in ADLB (35%), DLB (35%), and PSP (30%) (Fig. 2A). The soluble fraction showed significant decrease in levels of pan 14-3-3s in AD (34%), ADLB (35%), and DLB (36%) (Fig. 2B). Pan 14-3-3 levels in the insoluble fraction were elevated in AD by 19% (Fig. 2B).

We performed linear regression to assess the influence of demographic factors, including age, gender, and apolipoprotein E (apoE) genotype, on all ten 14-3-3 measurements (pS232, pS58, pS185, total 14-3-3θ, and pan 14-3-3s in soluble and insoluble fractions). Disease group remained significant for nearly all 14-3-3 measures except for soluble 14-3-3θ and insoluble pS58, the 14-3-3

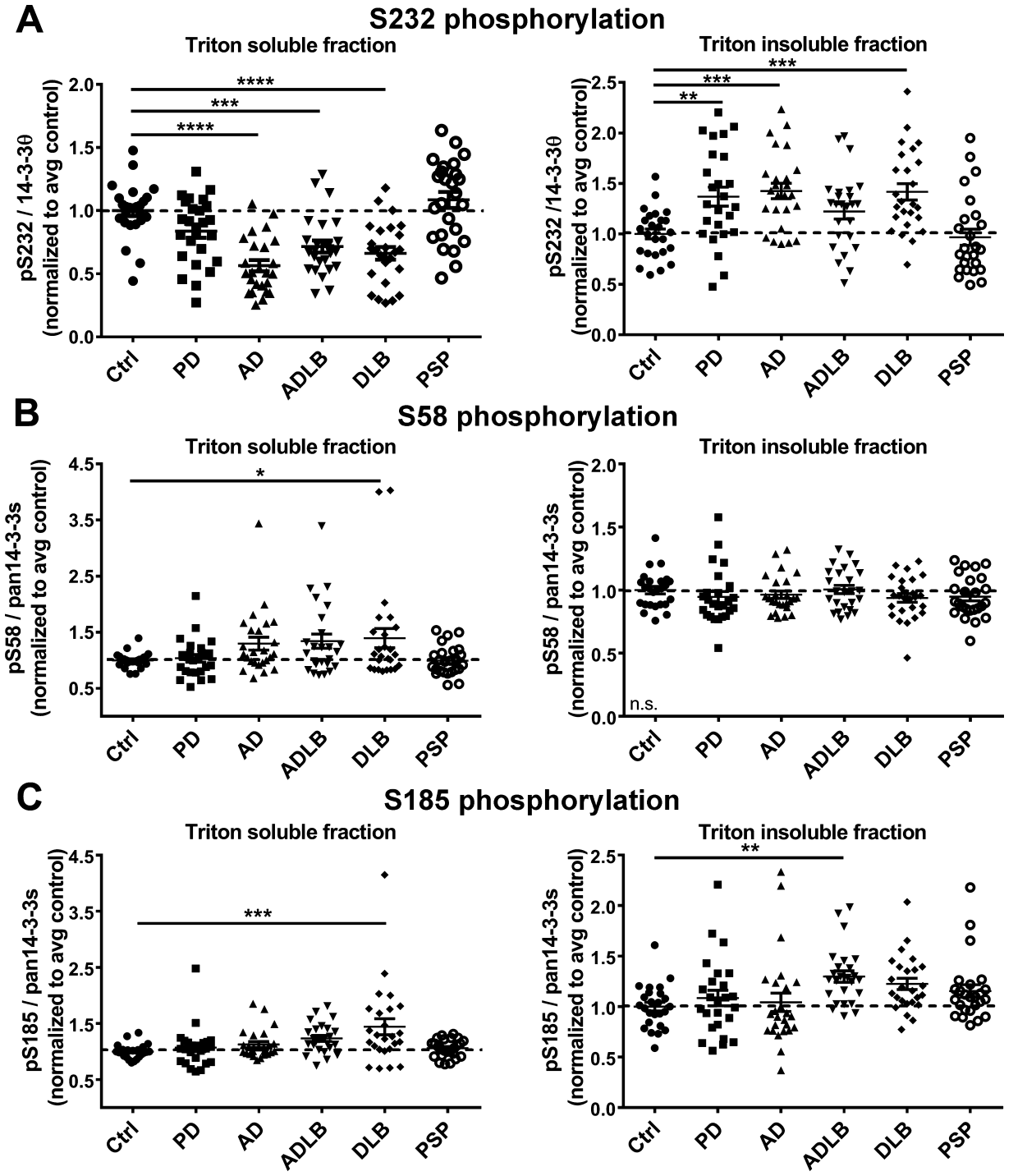

Figure 1. Serine 232 phosphorylation of 14-3-3θ is altered in several neurodegenerative disorders. (A) S232 phosphorylation was decreased in the soluble fraction in AD, ADLB, and DLB brains, but increased in the insoluble fraction in PD, AD, and DLB brains. Lysates of human temporal cortices were fractionated in Triton X-100 soluble and insoluble fractions and then analyzed for pS232 and total 14-3-3θ by western blot. The ratio of pS232 to total 14-3-3θ is quantified for 25 samples per group. (B) S58 phosphorylation was increased only in the soluble fraction in DLB samples. The ratio of pS58 to pan 14-3-3s is quantified for 25 samples per group. n.s.(nonsignificant). (C) S185 phosphorylation was significantly increased in the DLB group in the Triton X-100 soluble fraction, and increased in the insoluble fraction in the ADLB group. The ratio of pS185 to pan 14-3-3s is quantified for 25 samples per group. *$P < 0.05$, **$P < 0.01$, ***$P < 0.001$, ****$P < 0.0001$ compared to control (Dunnett's post hoc multiple comparison test).

Table 1. Mean and range of demographic and clinical characteristics of participants from whom brain samples were obtained.

Characteristic	Control (n = 25)	PD (n = 25)	AD (n = 25)	ADLB (n = 25)	DLB (n = 25)	PSP (n = 25)
No. male (%)	15 (60%)	17 (68%)	10 (40%)	12 (48%)	14 (56%)	15 (60%)
Age	81 (53–99)	81 (69–91)	82 (60–96)	83 (64–97)	76 (61–87)	84 (69–99)
Last MMSE score	28 (25–30)	21 (8–29)	12 (1–25)	13 (1–25)	13 (1–27)	23 (10–30)
	n = 14	n = 19	n = 21	n = 20	n = 19	n = 19
UPDRS score, off	10.6 (3–18)	53.6 (17–78)	14.7 (5–51)	30.5 (4–58.50)	50.0 (5.5–79)	34.9 (3–74.5)
	n = 13	n = 13	n = 7	n = 6	n = 7	n = 20

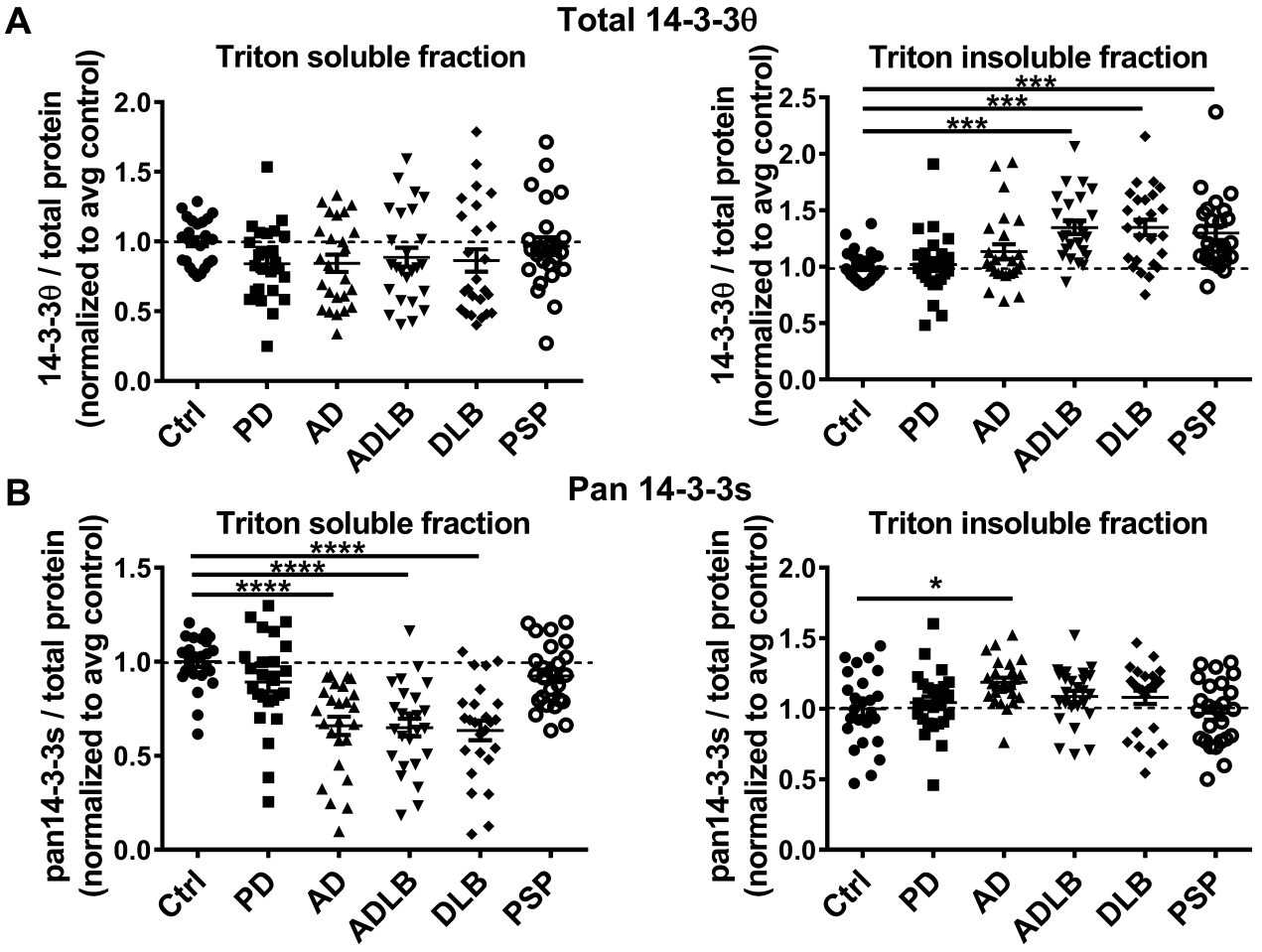

Figure 2. Soluble total 14-3-3 levels are reduced in AD, DLB, and ADLB brains. (A) Insoluble 14-3-3θ levels were significantly increased in DLB, ADLB, and PSP brain. 14-3-3θ was normalized to total protein loading as determined by EZBlue Protein Gel staining. n = 25 brains per group. (B) Soluble total 14-3-3s levels were significantly reduced in AD, DLB, and ADLB brains, and insoluble total 14-3-3s levels were increased in AD brains. Triton X-100 soluble and insoluble fraction lysates of human temporal cortices were analyzed for pan 14-3-3 by western blot. Pan 14-3-3 was normalized to total protein loading as determined by EZBlue Protein Gel staining. n = 25 brains per group. *$P < 0.05$, ***$P < 0.001$, ****$P < 0.0001$ compared to control (Dunnett's post hoc test). n.s.,nonsignificant.

measures that were not significant in the univariate ANOVA analyses. Demographic factors were not significantly associated with 14-3-3 measures in the combined model, except that apoE remained significantly associated with soluble pan 14-3-3 levels ($P < 0.05$). Age, while not achieving statistical significance possibly due to the restricted age range in these diseases of the elderly, was associated with S232 phosphorylation of 14-3-3θ in the insoluble fraction ($P = 0.055$), pointing to a potential independent role of age in S232 phosphorylation.

S232 phosphorylation of 14-3-3θ is associated with neurons

14-3-3 proteins are highly expressed throughout the brain, with high levels associated with neurons, but expression is also detected in glial cells and endothelial cells.[32–37] We performed immunohistochemistry on free-floating sections from control brains and brains with both AD and PD pathology to determine which cell populations expressed 14-3-3s and S232 phosphorylation. Immunohistochemistry using a monoclonal antibody against pan 14-3-3s demonstrated diffuse expression throughout the temporal cortical sections from control brains (Fig. 3A–C). Pan 14-3-3 staining was

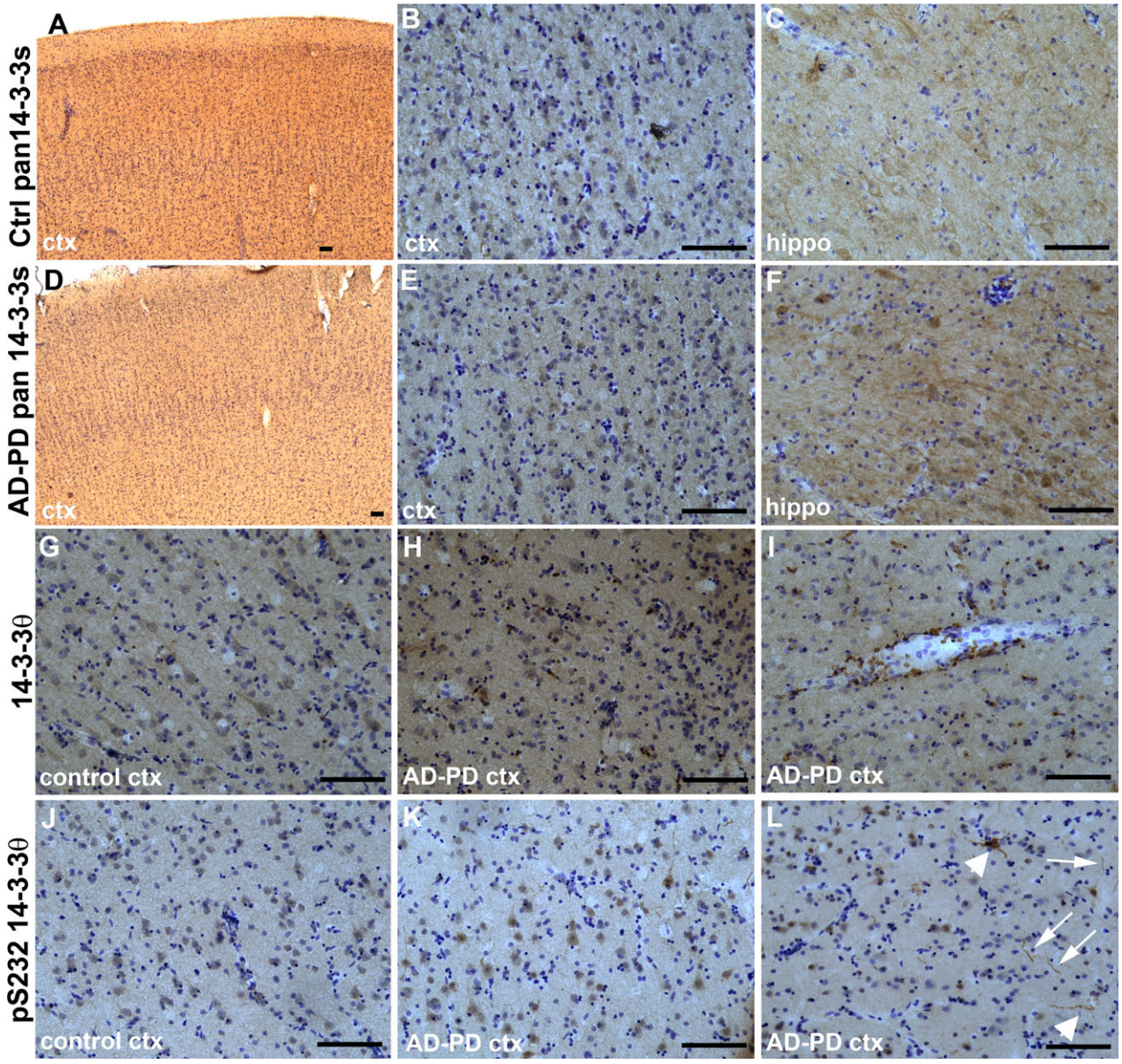

Figure 3. 14-3-3 expression and S232 phosphorylation are associated with neuronal cell bodies and neuropil. (A–F) Immunohistochemistry against pan 14-3-3 proteins in temporal cortical sections reveals diffuse staining for pan 14-3-3s in the neuropil and neuronal cell bodies in cortex (A, B, D, E) and hippocampus (C, F) in control brains and brains with both AD and PD pathology. (G–I) 14-3-3θ staining is found in neurons and neuropil in both control (G) and disease (H) brain sections. Staining of cells within blood vessels (I) was also observed in some control and disease brain sections. (J–L) Staining for pS232 14-3-3θ in temporal cortex reveals strong immunoreactivity in neurons and some staining in neuropil in control brains (J) and in AD-PD brains (K). Highly intense immunoreactivity is observed occasionally in neuritic structures and in neurons in AD-PD brains (L; arrowheads point to intense neuronal staining; arrows point to intense neuritic structures). Scale bars = 100 μm.

predominantly found in the neuropil but staining of neuronal cell bodies was also noted, particularly in the hippocampus (Fig. 3A–C). Similar pan 14-3-3 immunoreactivity was noted in temporal cortical sections from brains with pathological diagnoses of both AD and PD (Fig. 3D–F). Immunohistochemistry using a monoclonal antibody against 14-3-3θ showed a similar pattern with diffuse staining in the neuropil and neuronal cell bodies in sections from control brains and brains with AD and PD pathology (Fig. 3G and H). Some control and disease brain sections also demonstrated 14-3-3θ immunoreactivity associated with blood vessels (Fig. 3I). Immunohistochemistry for pS232 14-3-3θ showed prominent staining associated with neurons and neuropil in control and AD-PD brains (Fig. 3J and K). In addition, very intense, dark staining of neuritic-like structures and neurons that appeared possibly degenerating was occasionally observed in sections from all five out of five AD-PD brains examined (Fig. 3L); intense staining of neuritic-like structures was very rarely observed in sections from only two out of five control brains, and this intense, dark neuronal staining was not noted in these five control brains. This finding suggests that pS232 may be associated with insoluble protein aggregates in disease brains.

S232 phosphorylation is associated with solubility of 14-3-3s

Our western blot analysis showed that S232 phosphorylation was reduced in the soluble fraction but increased in the insoluble fraction in AD, ADLB, PD, and DLB, as emphasized by the ratio of soluble pS232 to insoluble pS232 in these disorders (Fig. 4A). In these same disorders, we observed a reduction in soluble pan 14-3-3 levels (Fig. 2B). We examined whether S232 phosphorylation was associated with soluble pan 14-3-3 levels. Lower log soluble/insoluble pS232 ratios, pointing to higher pS232 in the insoluble fraction, were associated with lower soluble pan 14-3-3 levels in a model unadjusted for disease group (Fig. 4B). Similar associations between the log of soluble/insoluble pS232 ratios and soluble pan 14-3-3 levels were also observed for each disease group except for PSP (Table S1). This association suggests that S232 phosphorylation could underlie the insolubilization of 14-3-3s.

S232 phosphorylation is associated with clinical and pathological severity

We next tested whether S232 phosphorylation or soluble 14-3-3 levels were associated with disease severity, as measured by clinical or pathological scores. We first examined whether the soluble to insoluble pS232 ratio or soluble pan 14-3-3 levels correlated with either the motor United Parkinson's Disease Rating Scale (UPDRS) or the Mini Mental Status Examination (MMSE) score. "Off" motor UPDRS score did not correlate with either 14-3-3 measure, whether unadjusted or adjusted for disease group. Of note, "off" motor UPDRS scores were available in only 68/150 subjects (45%). Higher MMSE scores correlated with higher log soluble pS232/insoluble pS232 ratios and with higher soluble pan 14-3-3 levels in a model unadjusted for group (Fig. 5).

We also examined whether the soluble/insoluble pS232 ratio or soluble pan 14-3-3 levels correlated with plaque density, tangle density, and Lewy-related histopathology

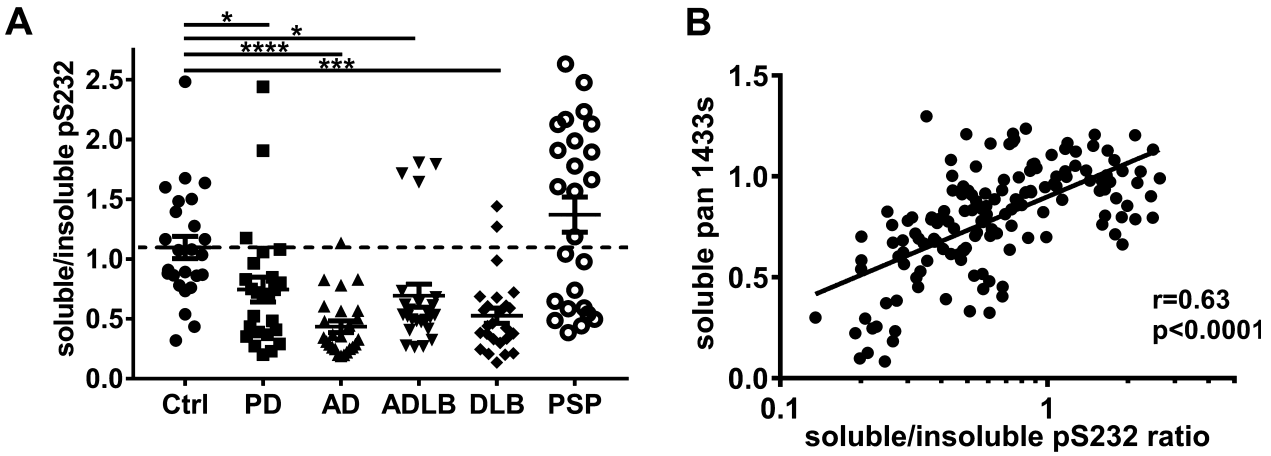

Figure 4. Soluble/insoluble pS232 ratios correlate with soluble 14-3-3 levels. (A) The ratio of soluble pS232 to insoluble pS232 14-3-3θ was significantly reduced in PD, AD, ADLB, and DLB brains. $n = 25$ brains per group. *$P < 0.05$, ***$P < 0.001$, ****$P < 0.0001$ compared to control (Dunnett's post hoc test). (B) Lower soluble to insoluble pS232 ratios were correlated with lower soluble pan 14-3-3 levels. Pearson correlation was performed to test the association between the log soluble/insoluble pS232 ratio and soluble pan 14-3-3 levels. $n = 150$.

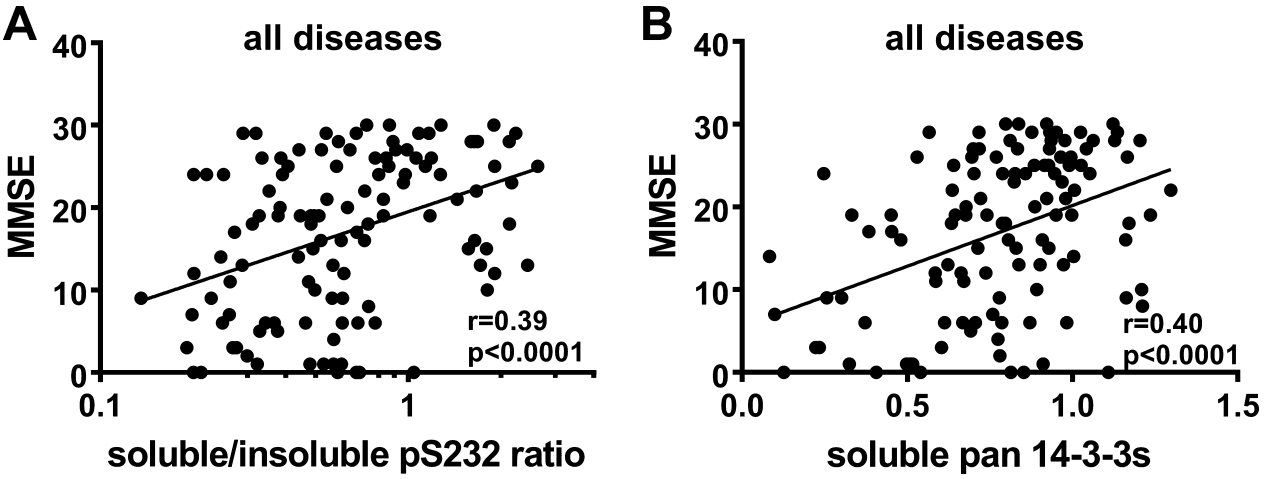

Figure 5. Soluble/insoluble pS232 ratio and soluble pan 14-3-3s levels correlate with MMSE scores. (A) Lower soluble to insoluble pS232 ratios were correlated with lower MMSE scores. Pearson correlation was performed to test the association between the log pS232 ratio and MMSE scores across all brains from which last MMSE score was documented prior to death. $n = 118$. (B) Lower soluble pan 14-3-3 levels were correlated with lower MMSE scores. Pearson correlation was performed to test the association between soluble pan 14-3-3 levels and MMSE scores across all brains from which last MMSE score was documented prior to death. $n = 118$. Mini MMSE, Mental Status Examination.

scores, using Spearman's rank correlation analysis. In a model unadjusted for group, lower log soluble pS232/insoluble pS232 ratios correlated modestly with higher temporal plaque density ($r = -0.32$, $P < 0.0001$), higher temporal tangle density ($r = -0.35$, $P < 0.0001$), and higher temporal Lewy-related density scores ($r = -0.26$, $P = 0.0014$). Lower soluble pan 14-3-3 levels also correlated with higher temporal plaque density ($r = -0.41$, $P < 0.0001$), higher temporal tangle density ($r = -0.45$, $P < 0.0001$), and higher temporal Lewy-related density scores ($r = -0.26$, $P = 0.0012$). We also measured phospho-S129 αsyn levels in the insoluble brain lysates by western blot as a separate measure of αsyn pathology and Aβ42 levels in the insoluble brain lysates by ELISA as a separate measure of Aβ pathology. Higher insoluble pS129 αsyn levels similarly correlated modestly with lower log soluble pS232/insoluble pS232 ratios ($r = -0.29$, $P = 0.0012$) and with lower soluble pan 14-3-3 levels ($r = -0.28$, $P = 0.0021$). Higher insoluble Aβ42 levels correlated modestly with lower log soluble pS232/insoluble pS232 ratios ($r = -0.23$, $P < 0.0001$) and with lower soluble pan 14-3-3 levels ($r = -0.39$, $P < 0.0001$). These data suggest that aggregation-related pathology may promote 14-3-3 insolubilization or that lower soluble pan 14-3-3s promotes aggregation of other neurodegeneration-related proteins.

Discussion

In this study, we examined the phosphorylation state of three conserved sites on 14-3-3s in postmortem temporal cortex of control, PD, AD, ADLB, DLB, and PSP subjects. We found that the S232 phosphorylation of 14-3-3θ was dramatically decreased in the soluble fraction but increased in the insoluble fraction in PD, AD, ADLB, and DLB brains. S185 phosphorylation was increased in DLB brains in the soluble fraction and increased in the insoluble fraction of ADLB brains. S58 phosphorylation was increased only in DLB brains in the soluble fraction. No phosphorylation changes at any site were observed in PSP samples. Additionally, pan 14-3-3 levels were significantly decreased for AD, ADLB, and DLB brains in the soluble fraction, while in the insoluble fraction, pan 14-3-3 levels were significantly increased in AD. 14-3-3θ levels were also increased in the insoluble fraction in ADLB, DLB, and PSP brains, suggesting that 14-3-3θ may be preferentially insolubilized.

High levels of 14-3-3s are primarily expressed in neurons, but expression of 14-3-3s is detectable in non-neuronal populations, including glial and endothelial cells.[32–37] As our western blot analysis cannot distinguish whether 14-3-3s were associated with neurons or other non-neuronal cells, we performed immunohistochemistry for 14-3-3s on sections from control brains and brains with both AD and PD pathology. Immunoreactivity against pan 14-3-3s was found predominantly in the neuropil and in neuronal cell bodies in control and diseased brains, although staining of non-neuronal cells could not be excluded. 14-3-3θ immunoreactivity was also found in neurons and neuropil in sections from control and disease brains, and some control and PD-AD brain sections also demonstrated immunoreactivity associated with

blood vessels. This immunoreactivity may be localized to red blood cells, as the staining was limited to non-nucleated cells within vessel lumen. PS232 immunoreactivity was most prominently associated with neurons and to a lesser degree with neuropil. Additionally, in sections from all five diseased brains, we observed occasional but very intense staining of neuritic processes and neuronal cell bodies that resembled protein-aggregate-like pathology. Intense neuritic staining was very rarely noted in sections from only two out of five control brains. This staining pattern is consistent with our western blot data in which S232 phosphorylation is associated with insoluble protein fractions. Overall, our immunostaining studies suggest that the changes in pS232 and soluble pan 14-3-3s are most likely related to neuronal alterations in 14-3-3s, although contribution from glial or endothelial cells cannot be ruled out.

A key finding of our study was the clear decrease in pS232 in the soluble fraction with a converse increase in pS232 in the insoluble fraction for diseases associated with Lewy body or Alzheimer pathology. The ratio of soluble to insoluble pS232 (Fig. 4A) highlights a redistribution of phosphorylated 14-3-3θ at S232 into the insoluble fraction. This dramatic change in S232 phosphorylation among several neurodegenerative diseases suggests that this phosphorylation site is of pathological significance in neurodegeneration. We have previously shown that S232 phosphorylation is altered in PD models: αsyn overexpression induces increased S232 phosphorylation, and rotenone causes a biphasic response with an initial increase followed by a decrease in S232 phosphorylation.[31] Increased S232 phosphorylation is associated with loss of neuroprotective function in in vitro PD models: the phosphomimetic S232D mutant failed to protect against rotenone or MPP^+ toxicity, while the nonphosphorylatable S232A mutant showed increased neuroprotection compared to wildtype 14-3-3θ[31]. Based on our previous work[31], we predict that changes in pS232 observed in these human brains contribute to neuronal loss in these disorders.

Our data also suggest that the S232 phosphorylation site could serve as a regulatory site for the solubility of 14-3-3s. We found that the ratio of soluble pS232 to insoluble pS232 correlated strongly with soluble 14-3-3 levels (Fig. 4B). The lower the soluble to insoluble pS232 ratio (equivalent to higher insoluble pS232 relative to soluble pS232), the lower the soluble 14-3-3 levels are. This correlation points to the possibility that S232 phosphorylation regulates 14-3-3 solubility. As 14-3-3s become phosphorylated at S232, it may partition more into the detergent insoluble fraction, thus resulting in lower levels of soluble 14-3-3s. Our cross-sectional data cannot point to whether phosphorylation or insolubilization occurs first, so the question remains if S232 phosphorylation causes 14-3-3s to partition into the insoluble fraction or if 14-3-3s are phosphorylated at serine 232 because they are associated with insoluble aggregates. Of note, we observed insolubilization of several 14-3-3 isoforms while S232 phosphorylation is specific to 14-3-3θ. As 14-3-3θ can heterodimerize with other isoforms[38–40], these findings suggest that increased S232 phosphorylation of 14-3-3θ may be sufficient to drive insolubilization of other isoforms through heterodimerization.

Insolubility of 14-3-3s is critical as only the soluble form of 14-3-3s is likely biologically active. Given 14-3-3s' key role in cell survival, low levels of soluble, and thus functional, 14-3-3s would be predicted to promote neuronal loss. Inhibition of 14-3-3s promotes cell loss in several PD models, while overexpression of 14-3-3s, in particular 14-3-3θ, reduces toxicity in several PD models.[5,15–17] 14-3-3s also impact neurite growth, spine density, and cognitive function: a functional 14-3-3 knockout demonstrates reduced dendritic length and spine numbers, reduced impaired long-term potentiation, and abnormalities in contextual fear conditioning.[5,41,42] The loss of soluble 14-3-3s observed here may contribute to synapse loss and cognitive decline. Consistent with this, we observed a correlation between soluble 14-3-3 levels and MMSE scores. Another consequence of reduced soluble 14-3-3 levels is impairment of 14-3-3s' chaperone function.[2,43,44] As several of 14-3-3s' interactors include key aggregation-prone proteins implicated in neurodegeneration, such as αsyn or Aβ, loss of soluble 14-3-3s and thus loss of chaperone function could promote aggregation and insolubilization of these proteins. Indeed, 14-3-3s reduce αsyn fibrillization, but this chaperone function can be overcome when 14-3-3 levels are low relative to αsyn.[43] Consistent with this idea, we did observe that lower soluble pan 14-3-3 levels correlated with higher αsyn-related tangle, or plaque pathology, suggesting that aggregation-related pathology is associated with 14-3-3 insolubilization. From our cross-sectional data, we cannot know whether lower soluble 14-3-3s or increased Lewy body or Alzheimer pathology occurred first; therefore, it is possible that αsyn or Aβ aggregation causes sequestration and insolubilization of 14-3-3s and/or that lower soluble 14-3-3s promotes further aggregation of Aβ and αsyn.

14-3-3s role in neurodegeneration may not be simply protective in all neurodegenerative disorders. It is alternatively possible that 14-3-3s could promote neurodegeneration under certain conditions. Previous studies have shown that 14-3-3ζ can bind tau and promote tau phosphorylation and aggregation in vitro.[22,45–47] In this scenario, the reduction in 14-3-3 soluble levels that we

observed could be compensatory in order to reduce any pro-aggregation effect that 14-3-3s may have on tau or other proteins.

Besides S232, we also evaluated phosphorylation at S58 and S185, two other conserved 14-3-3 phosphorylation sites. We observed subtle but significant alterations in S58 and S185 phosphorylation in DLB and/or ADLB brains. The lack of changes at these two other sites in most diseases examined suggests that only S232 phosphorylation serves as a common mechanism for neurodegeneration. However, these data imply that these other phosphorylation changes could be specific to DLB pathophysiology, and that S185 and S58 phosphorylation could possibly distinguish DLB from other neurodegenerative disorders that can be difficult to distinguish clinically, particularly early in the disease course.

We did not observe any changes in 14-3-3s in PSP for the most part. This suggests that 14-3-3 does not play a role in PSP pathophysiology. This disorder is quite distinct clinically and pathologically from those disorders marked by αsyn or plaque pathology. It should be noted that we had access to only temporal cortex samples for analysis. Therefore, the lack of changes in pS232 observed in PSP and the milder change in PD brains could be secondary to the brain region examined in our study and not necessarily reflective of the pathological changes observed in the disorder itself. Sampling of different brain regions, such as the substantia nigra, may have revealed more prominent S232 changes in PD or PSP. It is also possible that a more dramatic phenotype in temporal cortical samples may have been noted if obtained from brains at later stages of disease.

We used postmortem temporal cortical tissue for our 14-3-3 analyses. If similar changes are detectable in more easily accessible biospecimens, including CSF and plasma, 14-3-3 phosphorylation has the potential as a biomarker for neurodegeneration. Measurement of 14-3-3s in CSF has been used clinically as a diagnostic biomarker for Creutzfeldt-Jakob Disease (CJD), although recent studies have demonstrated that the specificity for CJD is lower than initially thought.[48–51] However, this body of research has demonstrated that 14-3-3 measurements in CSF are reliable and stable in patients, and can help with diagnosis in the right clinical context.[48,49] Further evaluation of 14-3-3 phosphorylation in CSF and plasma is indicated for these disorders.

In conclusion, S232 phosphorylation and soluble 14-3-3 levels are altered in neurodegenerative disorders associated with Lewy body or Alzheimer's pathology. This phosphorylation change may underlie the insolubilization of 14-3-3 proteins observed in these disorders, and loss of 14-3-3 function may make a critical contribution to the pathophysiology of these diseases.

Acknowledgments

This work was supported by the Michael J. Fox Foundation for Parkinson's Research, the National Institute of Neurological Disorders and Stroke (R01 NS088533), and the Parkinson's Association of Alabama. We are grateful to the Banner Sun Health Research Institute Brain and Body Donation Program of Sun City, Arizona for the provision of human brain tissue. The Brain and Body Donation Program is supported by the National Institute on Aging (P30 AG19610 Arizona Alzheimer's Disease Core Center), the Arizona Department of Health Services (contract 211002, Arizona Alzheimer's Research Center), the Arizona Biomedical Research Commission (contracts 4001, 0011, 05-901 and 1001 to the Arizona Parkinson's Disease Consortium) and the Prescott Family Initiative of the Michael J. Fox Foundation for Parkinson's Research.

Conflict of Interest

Michael McFerrin and Xiaofei Chi have no potential conflicts of interest to declare. Gary Cutter serves on Data and Safety Monitoring Boards for AMO Pharma, Apotek, Gilead Pharmaceuticals, Horizon Pharmaceuticals, Modigenetech/Prolor, Merck, Merck/Pfizer, Opko Biologics, Neuren, Sanofi-Aventis, Reata Pharmaceuticals, Receptos/Celgene, Teva pharmaceuticals, NHLBI (Protocol Review Committee), NICHD (OPRU oversight committee). He serves on Consulting or Advisory Boards for Cerespir Inc, Consortium of MS Centers (grant), Genzyme, Genentech, Innate Therapeutics, Jannsen Pharmaceuticals, Klein-Buendel Incorporated, Medimmune, Medday, Nivalis, Novartis, Opexa Therapeutics, Roche, Savara Inc., Somahlution, Teva pharmaceuticals, Transparency Life Sciences, and TG Therapeutics. Dr. Cutter is employed by the University of Alabama at Birmingham and President of Pythagoras, Inc. a private consulting company located in Birmingham AL. Talene Yacoubian has a U.S. Patent #7,919,262 on the use of 14-3-3s in neurodegeneration. She has received grant funding from the American Parkinson Disease Association, Michael J. Fox Foundation, Parkinson Association of Alabama, Alzheimer's of Central Alabama, Alabama Drug Discovery Alliance, and NIH in the last 3 years. Dr. Yacoubian has a clinical practice and is compensated for these activities through the University of Alabama Health Services Foundation. She has received honoraria and travel support for presentations and grant reviews from the Movement Disorders Society, NIH, and the Michael J. Fox Foundation in the last 3 years.

References

1. Dougherty MK, Morrison DK. Unlocking the code of 14-3-3. J Cell Sci 2004;117(Pt 10):1875–1884.
2. Yano M, Nakamuta S, Wu X, et al. A novel function of 14-3-3 protein: 14-3-3zeta is a heat-shock-related molecular chaperone that dissolves thermal-aggregated proteins. Mol Biol Cell 2006;17:4769–4779.
3. Mrowiec T, Schwappach B. 14-3-3 proteins in membrane protein transport. Biol Chem 2006;387:1227–1236.
4. Porter GW, Khuri FR, Fu H. Dynamic 14-3-3/client protein interactions integrate survival and apoptotic pathways. Semin Cancer Biol 2006;16:193–202.
5. Lavalley NJ, Slone SR, Ding H, et al. 14-3-3 Proteins regulate mutant LRRK2 kinase activity and neurite shortening. Hum Mol Genet 2016;25:109–122.
6. Yoon BC, Zivraj KH, Strochlic L, Holt CE. 14-3-3 proteins regulate retinal axon growth by modulating ADF/cofilin activity. Developmental Neurobiol. 2012;72:600–614.
7. Ostrerova N, Petrucelli L, Farrer M, et al. alpha-Synuclein shares physical and functional homology with 14-3-3 proteins. J Neurosci 1999;19:5782–5791.
8. Xu J, Kao SY, Lee FJ, et al. Dopamine-dependent neurotoxicity of alpha-synuclein: a mechanism for selective neurodegeneration in Parkinson disease. Nat Med 2002;8:600–606.
9. Sato S, Chiba T, Sakata E, et al. 14-3-3eta is a novel regulator of parkin ubiquitin ligase. EMBO J 2006;25:211–221.
10. Li X, Wang QJ, Pan N, et al. Phosphorylation-dependent 14-3-3 binding to LRRK2 is impaired by common mutations of familial Parkinson's disease. PLoS ONE 2011;6:e17153.
11. Nichols RJ, Dzamko N, Morrice NA, et al. 14-3-3 binding to LRRK2 is disrupted by multiple Parkinson's disease-associated mutations and regulates cytoplasmic localization. Biochem. J. 2010;430:393–404.
12. Kawamoto Y, Akiguchi I, Nakamura S, et al. 14-3-3 proteins in Lewy bodies in Parkinson disease and diffuse Lewy body disease brains. J Neuropathol Exp Neurol 2002;61:245–253.
13. Berg D, Riess O, Bornemann A. Specification of 14-3-3 proteins in Lewy bodies. Ann Neurol 2003;54:135.
14. Ding H, Fineberg NS, Gray M, Yacoubian TA. alpha-Synuclein overexpression represses 14-3-3theta transcription. J Mol Neurosci 2013;51:1000–1009.
15. Yacoubian TA, Slone SR, Harrington AJ, et al. Differential neuroprotective effects of 14-3-3 proteins in models of Parkinson's disease. Cell Death Dis 2010;1:e2.
16. Ding H, Underwood R, Lavalley N, Yacoubian TA. 14-3-3 inhibition promotes dopaminergic neuron loss and 14-3-3theta overexpression promotes recovery in the MPTP mouse model of Parkinson's disease. Neuroscience 2015;307:73–82.
17. Slone SR, Lesort M, Yacoubian TA. 14-3-3theta Protects against Neurotoxicity in a Cellular Parkinson's Disease Model through Inhibition of the Apoptotic Factor Bax. PLoS ONE 2011;6:e21720.
18. Sumioka A, Nagaishi S, Yoshida T, et al. Role of 14-3-3gamma in FE65-dependent gene transactivation mediated by the amyloid beta-protein precursor cytoplasmic fragment. J Biol Chem 2005;280:42364–42374.
19. Shirasaki DI, Greiner ER, Al-Ramahi I, et al. Network organization of the huntingtin proteomic interactome in mammalian brain. Neuron 2012;75:41–57.
20. Okamoto Y, Shirakashi Y, Ihara M, et al. Colocalization of 14-3-3 proteins with SOD1 in Lewy body-like hyaline inclusions in familial amyotrophic lateral sclerosis cases and the animal model. PLoS ONE 2011;6:e20427.
21. Omi K, Hachiya NS, Tanaka M, et al. 14-3-3zeta is indispensable for aggregate formation of polyglutamine-expanded huntingtin protein. Neurosci Lett 2008;24 (431):45–50.
22. Sadik G, Tanaka T, Kato K, et al. Phosphorylation of tau at Ser214 mediates its interaction with 14-3-3 protein: implications for the mechanism of tau aggregation. J Neurochem 2009;108:33–43.
23. Liao L, Cheng D, Wang J, et al. Proteomic characterization of postmortem amyloid plaques isolated by laser capture microdissection. J Biol Chem 2004;279:37061–37068.
24. Umahara T, Uchihara T, Tsuchiya K, et al. 14-3-3 proteins and zeta isoform containing neurofibrillary tangles in patients with Alzheimer's disease. Acta Neuropathol 2004;108:279–286.
25. Waelter S, Boeddrich A, Lurz R, et al. Accumulation of mutant huntingtin fragments in aggresome-like inclusion bodies as a result of insufficient protein degradation. Mol Biol Cell 2001;12:1393–1407.
26. Woodcock JM, Murphy J, Stomski FC, et al. The dimeric versus monomeric status of 14-3-3zeta is controlled by phosphorylation of Ser58 at the dimer interface. J Biol Chem 2003;278:36323–36327.
27. Sunayama J, Tsuruta F, Masuyama N, Gotoh Y. JNK antagonizes Akt-mediated survival signals by phosphorylating 14-3-3. J Cell Biol 2005;170:295–304.
28. Yoshida K, Yamaguchi T, Natsume T, et al. JNK phosphorylation of 14-3-3 proteins regulates nuclear targeting of c-Abl in the apoptotic response to DNA damage. Nat Cell Biol 2005;7:278–285.
29. Zhou J, Shao Z, Kerkela R, et al. Serine 58 of 14-3-3zeta is a molecular switch regulating ASK1 and oxidant stress-induced cell death. Mol Cell Biol 2009;29:4167–4176.
30. Obsilova V, Herman P, Vecer J, et al. 14-3-3zeta C-terminal stretch changes its conformation upon ligand binding and phosphorylation at Thr232. J Biol Chem 2004;279:4531–4540.

31. Slone SR, Lavalley N, McFerrin M, et al. Increased 14-3-3 phosphorylation observed in Parkinson's disease reduces neuroprotective potential of 14-3-3 proteins. Neurobiol Dis 2015;79:1–13.
32. Baxter HC, Liu WG, Forster JL, et al. Immunolocalisation of 14-3-3 isoforms in normal and scrapie-infected murine brain. Neuroscience 2002;109:5–14.
33. Umahara T, Uchihara T, Nakamura A, Iwamoto T. Differential expression of 14-3-3 protein isoforms in developing rat hippocampus, cortex, rostral migratory stream, olfactory bulb, and white matter. Brain Res 2011;1410:1–11.
34. VanGuilder HD, Farley JA, Yan H, et al. Hippocampal dysregulation of synaptic plasticity-associated proteins with age-related cognitive decline. Neurobiol Dis 2011;43:201–212.
35. Watanabe M, Isobe T, Ichimura T, et al. Molecular cloning of rat cDNAs for beta and gamma subtypes of 14-3-3 protein and developmental changes in expression of their mRNAs in the nervous system. Brain Res Mol Brain Res 1993;17(1–2):135–146.
36. Watanabe M, Isobe T, Ichimura T, et al. Molecular cloning of rat cDNAs for the zeta and theta subtypes of 14-3-3 protein and differential distributions of their mRNAs in the brain. Brain Res Mol Brain Res 1994;25(1–2):113–121.
37. Watanabe M, Isobe T, Okuyama T, et al. Molecular cloning of cDNA to rat 14-3-3 eta chain polypeptide and the neuronal expression of the mRNA in the central nervous system. Brain Res Mol Brain Res 1991;10:151–158.
38. Chaudhri M, Scarabel M, Aitken A. Mammalian and yeast 14-3-3 isoforms form distinct patterns of dimers in vivo. Biochem Biophys Res Commun 2003;300:679–685.
39. Jones DH, Ley S, Aitken A. Isoforms of 14-3-3 protein can form homo- and heterodimers in vivo and in vitro: implications for function as adapter proteins. FEBS Lett 1995;368:55–58.
40. Yang X, Lee WH, Sobott F, et al. Structural basis for protein-protein interactions in the 14-3-3 protein family. Proc Natl Acad Sci USA 2006;103:17237–17242.
41. Qiao H, Foote M, Graham K, et al. 14-3-3 proteins are required for hippocampal long-term potentiation and associative learning and memory. J Neurosci 2014;34:4801–4808.
42. Foote M, Qiao H, Graham K, et al. Inhibition of 14-3-3 Proteins Leads to Schizophrenia-Related Behavioral Phenotypes and Synaptic Defects in Mice. Biol Psychiat 2015;78:386–395.
43. Plotegher N, Kumar D, Tessari I, et al. The chaperone-like protein 14-3-3eta interacts with human alpha-synuclein aggregation intermediates rerouting the amyloidogenic pathway and reducing alpha-synuclein cellular toxicity. Hum Mol Genet 2014;23:5615–5629.
44. Vincenz C, Dixit VM. 14-3-3 proteins associate with A20 in an isoform-specific manner and function both as chaperone and adapter molecules. J Biol Chem 1996;271:20029–20034.
45. Hashiguchi M, Sobue K, Paudel HK. 14-3-3zeta is an effector of tau protein phosphorylation. J Biol Chem 2000;275:25247–25254.
46. Qureshi HY, Han D, MacDonald R, Paudel HK. Overexpression of 14-3-3z promotes tau phosphorylation at Ser262 and accelerates proteosomal degradation of synaptophysin in rat primary hippocampal neurons. PLoS ONE 2013;8:e84615.
47. Qureshi HY, Li T, MacDonald R, et al. Interaction of 14-3-3zeta with microtubule-associated protein tau within Alzheimer's disease neurofibrillary tangles. Biochemistry 2013;52:6445–6455.
48. Muayqil T, Gronseth G, Camicioli R. Evidence-based guideline: diagnostic accuracy of CSF 14-3-3 protein in sporadic Creutzfeldt-Jakob disease: report of the guideline development subcommittee of the American Academy of Neurology. Neurology 2012;79:1499–1506.
49. Stoeck K, Sanchez-Juan P, Gawinecka J, et al. Cerebrospinal fluid biomarker supported diagnosis of Creutzfeldt-Jakob disease and rapid dementias: a longitudinal multicentre study over 10 years. Brain 2012;135(Pt 10):3051–3061.
50. Zerr I, Bodemer M, Gefeller O, et al. Detection of 14-3-3 protein in the cerebrospinal fluid supports the diagnosis of Creutzfeldt-Jakob disease. Ann Neurol 1998;43:32–40.
51. Burkhard PR, Sanchez JC, Landis T, Hochstrasser DF. CSF detection of the 14-3-3 protein in unselected patients with dementia. Neurology 2001;56:1528–1533.

Supporting Information

Additional Supporting Information may be found online in the supporting information tab for this article:

Figure S1. Representative western blot images of brain lysates probed for phosphorylated 14-3-3s and total 14-3-3s.

Figure S2. Immunohistochemistry of control brain sections without primary antibodies.

Table S1. Correlation between soluble/insoluble pS232 and soluble pan 14-3-3 levels within a given disease group.

